

Integrated GPS/INS Navigation System Based on a Gyroscope-Free IMU

Edmundo A. Marques Filho ¹, Helio Koiti Kuga ², Atair Rios Neto ³

¹ INPE, S. J. dos Campos, Brazil, edmonic@directnet.com.br

² INPE, S. J. dos Campos, Brazil, hkk@dem.inpe.br

³ INPE, S. J. dos Campos, Brazil, atairrn@uol.com.br

Abstract: This paper analyses the performance of a low cost INS, based on a gyro-free IMU that only uses multiples accelerometers and is aided by a GPS receiver. The IMU is composed by a specific array of accelerometers such that linear and angular accelerations can be computed. The GPS/INS loosely integration approach is implemented by a Kalman filter. The performance of the integrated system is assessed by using computer simulation.

Keywords: GPS/INS, gyro-free, Kalman.

1. INTRODUCTION

Inertial navigation systems (INS) are widely used in many applications including civilian and military aviation, spatial and nautical segments, automobiles, automated agricultural and construction vehicles, and robotics. Recent advances in MEMS (Micro Electro Mechanical System) technology have made inertial sensors more affordable and thus costs of micro-machined accelerometer and gyroscopes are decreasing while their performance characteristics are being improved [1], [2]. The INS gives the position, velocity and attitude but with growing time degradations due to sensor errors and random disturbances. Hence, an update or position fix can be taken from an external reference such as data from the GPS receiver. Micro-machined accelerometers are now in large-volume production, cost a few dollars and have been showing reliability, and so are GPS receivers, making a gyro-free GPS/INS attractive for low-cost, medium performance applications .

2. GYRO-FREE IMU CONFIGURATION

Standard inertial measurement unit, or IMU, uses accelerometers to sense linear accelerations and gyroscopes to sense angular velocity. A gyro-free IMU is a specific array of accelerometers where location and orientation are chosen in such way that angular and linear motions can be computed by using decoupled equations.

Since gyroscope's technology , besides its high cost, also suffers **commercial** restrictions, efforts to develop a gyro-free IMU have been done. Gyro-free IMU have been described by Pandgaonkar et alli [3], Merhav [4], Trabasso [5] and Chen et alii [6]. Gyro-free inertial navigation systems integrated with GPS are also described by Mostov et alii [7], Park e Tan [8] and Marques Filho [9].

In this paper a cube configuration with six accelerometers is used [6]. The array has one accelerometer

at the center of each face of the cube and the sensing axes are along the respective cube diagonal as shown in Figure 1 (adapted from [6]).

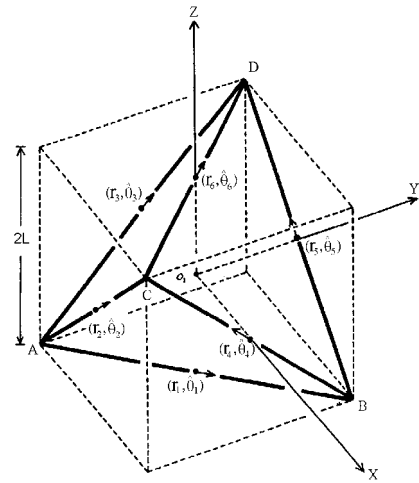


Fig. 1. Cube gyro-free IMU configuration

The equations of angular and linear accelerations are decoupled and are described with reference to the center of the cube, defined as the origin of the moving vehicle frame and are described by [6]:

$$\dot{\omega}_{iv}^v = \begin{bmatrix} \dot{\omega}_x \\ \dot{\omega}_y \\ \dot{\omega}_z \end{bmatrix} = \frac{1}{2L\sqrt{2}} \cdot \mathbf{J}_1 \cdot \begin{bmatrix} A_1 \\ A_2 \\ A_3 \\ A_4 \\ A_5 \\ A_6 \end{bmatrix}, \quad \omega_{iv}^v = \int \dot{\omega}_{iv}^v \quad (1)$$

$$\mathbf{f}^v = \begin{bmatrix} f_x \\ f_y \\ f_z \end{bmatrix} = \frac{1}{2\sqrt{2}} \cdot \mathbf{J}_2 \cdot \begin{bmatrix} A_1 \\ A_2 \\ A_3 \\ A_4 \\ A_5 \\ A_6 \end{bmatrix} + \mathbf{L} \begin{bmatrix} \omega_y \cdot \omega_z \\ \omega_z \cdot \omega_x \\ \omega_x \cdot \omega_y \end{bmatrix} \quad (2)$$

where:

2L is the cube height.

A_1, \dots, A_6 are the accelerometers outputs.

$\dot{\boldsymbol{\omega}}_{iv}^v$ are the angular accelerations of a vehicle frame (v) with relation to an inertial frame (i), and expressed in the vehicle frame.

\mathbf{f}^v are the linear accelerations or specific force of the vehicle frame (v).

\mathbf{J}_1 and \mathbf{J}_2 are matrices that define the accelerometer's location and orientation on cube faces and are described by:

$$\mathbf{J}_1 = \begin{bmatrix} 1 & -1 & 0 & 0 & 1 & -1 \\ -1 & 0 & 1 & -1 & 0 & -1 \\ 0 & 1 & -1 & -1 & 1 & 0 \end{bmatrix}, j=1, \dots, 6 \quad (3)$$

$$\mathbf{J}_2 = \begin{bmatrix} 1 & 1 & 0 & 0 & -1 & -1 \\ 1 & 0 & 1 & -1 & 0 & 1 \\ 0 & 1 & 1 & 1 & 1 & 0 \end{bmatrix}, j=1, \dots, 6 \quad (4)$$

3. GPS/INS INTEGRATION FILTER DESIGN

3.1 Inertial navigation equations

Strapdown inertial navigation algorithms consist of attitude, velocity and position equations that can be described in several references frames. The equations for the local tangent plane (LTP), or navigation frame, can be written as [10]:

$$\dot{\mathbf{r}}^n = \mathbf{v}^n \quad (5)$$

$$\dot{\mathbf{v}}^n = \mathbf{C}_v^n \cdot \mathbf{f}^v - (2\boldsymbol{\Omega}_{ie}^n + \boldsymbol{\Omega}_{en}^n) \cdot \mathbf{v}^n + \mathbf{g}^n \quad (6)$$

$$\dot{\mathbf{C}}_v^n = \mathbf{C}_v^n \cdot \boldsymbol{\Omega}_{nv}^v \quad (7)$$

where:

$\mathbf{r}^n = \{\Phi, \lambda, h\}$ is the position vector for latitude, longitude and height components,

$\mathbf{v}^n = \{\dot{\Phi}, \dot{\lambda}, \dot{h}\}$ is the velocity vector,

\mathbf{f}^n is the specific force vector, where $\mathbf{f}^n = \mathbf{C}_v^n \cdot \mathbf{f}^v$

\mathbf{C}_v^n is a transformation matrix from vehicle (v) to navigation (n) frame,

\mathbf{g}^n is the gravity vector,

$\boldsymbol{\Omega}$ denotes an angular velocity matrix

3.2 Inertial navigation error model

The Kalman Filtering technique, used to combine the inertial navigation solution and the GPS solution, requires error models of the INS and GPS systems. Perturbation method is used to linearize the nonlinear error equations [11,

12]. The (n x 1) state vector, \mathbf{x} , of the dynamical system is given by [9]:

$$\mathbf{x} = \{\delta \mathbf{r}^n, \delta \mathbf{v}^n, \boldsymbol{\varepsilon}^n, \delta \boldsymbol{\omega}_{iv}^v, \delta \mathbf{b}\} \quad (8)$$

where:

$\delta \mathbf{r}^n$ is the position error (3 x 1) vector,

$\delta \mathbf{v}^n$ is the velocity error (3 x 1) vector,

$\boldsymbol{\varepsilon}^n$ is the attitude error (3 x 1) vector,

$\delta \boldsymbol{\omega}_{iv}^v$ is the angular velocity error (3 x 1) vector and

$\delta \mathbf{b}$ is a lumped bias error (6 x 1) vector used to compensate for bias and scale factor errors from each IMU accelerometer output.

The error equations are given by [9,12]:

$$\delta \dot{\mathbf{r}}^n = \mathbf{F}_{rr} \cdot \delta \mathbf{r}^n + \mathbf{F}_{rv} \cdot \delta \mathbf{v}^n \quad (9)$$

Here, \mathbf{F}_{rr} and \mathbf{F}_{rv} are the matrices related to position errors given by [12]:

$$\mathbf{F}_{rr} = \begin{bmatrix} 0 & 0 & \frac{-v_N}{(R_M + h)^2} \\ \frac{v_E \cdot \sin \Phi}{(R_N + h) \cdot \cos^2 \Phi} & 0 & \frac{-v_E}{(R_N + h)^2 \cdot \cos \Phi} \\ 0 & 0 & 0 \end{bmatrix} \quad (10)$$

$$\mathbf{F}_{rv} = \begin{bmatrix} \frac{1}{(R_M + h)} & 0 & 0 \\ 0 & \frac{1}{(R_N + h) \cdot \cos \Phi} & 0 \\ 0 & 0 & -1 \end{bmatrix} \quad (11)$$

where v_E and v_N are the vehicle velocity east and north components, R_N is the transverse radius of curvature and R_M is the radius of curvature in a meridian at a given latitude, a is the equatorial radius and e is the eccentricity.

$$R_N = \frac{a}{(1 - e^2 \cdot \sin^2 \Phi)^{1/2}} \quad (12)$$

$$R_M = \frac{a(1 - e^2)}{(1 - e^2 \cdot \sin^2 \Phi)^{3/2}} \quad (13)$$

$$\delta \dot{\mathbf{v}}^n = \mathbf{F}_{vr} \cdot \delta \mathbf{r}^n + \mathbf{F}_{vv} \cdot \delta \mathbf{v}^n + \mathbf{f}^n \cdot \mathbf{E}^n + \mathbf{C}_v^n \cdot \delta \mathbf{f}^v \quad (14)$$

Here, \mathbf{F}_{vr} and \mathbf{F}_{vv} are the matrices related to velocity errors given by [9,12]:

$$\mathbf{F}_{vr} = \begin{bmatrix} -2v_E \omega_e \cdot \cos \Phi - v_E^2 / [(R_N + h) \cdot \cos^2 \Phi] & 0 \\ 2\omega_e (v_N \cos \Phi - v_D \sin \Phi) + v_E v_N / [(R_N + h) \cos^2 \Phi] & 0 \\ 2v_E \omega_e \cdot \sin \Phi & 0 \end{bmatrix} \quad (15)$$

$$\begin{bmatrix} -v_N v_D / (R_M + h)^2 + v_E^2 \tan \Phi / (R_N + h)^2 \\ -v_E v_D / (R_N + h)^2 - v_N v_E \tan \Phi / (R_N + h)^2 \\ v_E^2 / (R_N + h)^2 + v_N^2 / (R_M + h)^2 - \delta \mathbf{g}^n \end{bmatrix}$$

$$\mathbf{F}_{vv} = \begin{bmatrix} v_D / (R_M + h) & -2\omega_e \cdot \sin \Phi - 2v_E \cdot \tan \Phi / (R_N + h) \\ 2\omega_e \cdot \sin \Phi + v_E \cdot \tan \Phi / (R_N + h) & (v_D + v_N \cdot \tan \Phi) / (R_N + h) \\ -2v_N / (R_M + h) & (-2\omega_e \cdot \cos \Phi) - 2v_E / (R_N + h) \\ v_N / (R_M + h) \\ 2\omega_e \cdot \cos \Phi + v_E / (R_N + h) \\ 0 \end{bmatrix} \quad (16)$$

where v_D is the down velocity component, ω_e is the Earth rotation relative to inertial frame, $\delta \mathbf{g}^n$ is the gravitation errors and \mathbf{E}^n is the skew-symmetric matrix of attitude errors:

$$\mathbf{E}^n = \begin{bmatrix} 0 & -\varepsilon_D & \varepsilon_E \\ \varepsilon_D & 0 & -\varepsilon_N \\ -\varepsilon_E & \varepsilon_N & 0 \end{bmatrix} \quad (17)$$

$$\dot{\mathbf{e}}^n = \mathbf{F}_{er} \cdot \delta \mathbf{r}^n + \mathbf{F}_{ev} \cdot \delta \mathbf{v}^n - (\boldsymbol{\omega}_{in}^n \times) \mathbf{e}^n - \mathbf{C}_v^n \cdot \delta \boldsymbol{\omega}_{iv}^v \quad (18)$$

Here, \mathbf{F}_{er} and \mathbf{F}_{ev} are the matrices related to attitude errors given by [9,12] and $(\boldsymbol{\omega}_{in}^n \times)$ denotes the skew-symmetric matrix of the $\boldsymbol{\omega}_{in}^n$ components:

$$\mathbf{F}_{er} = \begin{bmatrix} -\omega_e \cdot \sin \Phi & 0 & -v_E / (R_N + h)^2 \\ 0 & 0 & v_N / (R_M + h)^2 \\ -\omega_e \cdot \cos \Phi - v_E / [(R_N + h) \cos^2 \Phi] & 0 & v_E \cdot \tan \Phi / (R_N + h)^2 \end{bmatrix} \quad (19)$$

$$\mathbf{F}_{ev} = \begin{bmatrix} 0 & 1 / (R_N + h) & 0 \\ -1 / (R_M + h) & 0 & 0 \\ 0 & -\tan \Phi / (R_N + h) & 0 \end{bmatrix} \quad (20)$$

$$\delta \boldsymbol{\omega}_{iv}^v = \frac{1}{2\sqrt{2} \cdot L} \cdot \mathbf{J}_1 \cdot \delta \mathbf{A} = \frac{1}{2\sqrt{2} \cdot L} \cdot \mathbf{J}_1 \cdot (\delta \mathbf{b} + \mathbf{w}_a) \quad (21)$$

$$\delta \mathbf{f}^v = \frac{1}{2\sqrt{2}} \cdot \mathbf{J}_2 (\delta \mathbf{b} + \mathbf{w}_a) + L \cdot \boldsymbol{\Omega} \cdot \delta \boldsymbol{\omega}_{iv}^v \quad (22)$$

$$\delta \mathbf{A} = \delta \mathbf{b} + \mathbf{w}_a \quad (23)$$

where $\delta \mathbf{A}$ is the vector of accelerometers errors, $\delta \mathbf{b}$ is the lumped bias error to be estimated by the Kalman filter and compensated on the accelerometers output during INS computations, and \mathbf{w}_a is a white noise.

$\delta \dot{\mathbf{b}} = \mathbf{w}_b$, \mathbf{w}_b is also modeled as white noise.

Equations (21) and (22) show that specific force and angular acceleration errors have the same source, the six accelerometers output. Finally,

$$\boldsymbol{\Omega} = \begin{bmatrix} 0 & \omega_z & \omega_y \\ \omega_z & 0 & \omega_x \\ \omega_y & \omega_x & 0 \end{bmatrix} \quad (24)$$

3.3 Kalman Filter Design

The Kalman filter algorithm is used to combine the inertial and GPS measurements in order to compensate for the errors included in INS model. Estimates of inertial error states are fed back to the INS algorithms to improve the navigation solution. Figure 2 shows a loosely coupled integrated configuration scheme where the GPS data is used as an external sensor [13].

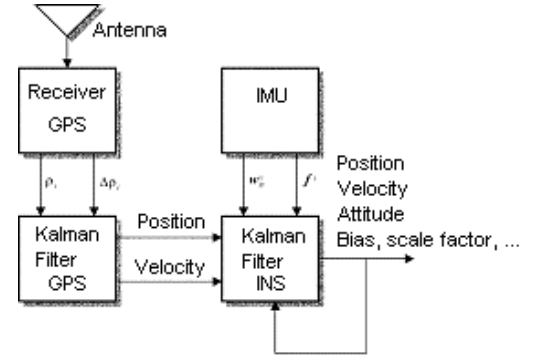


Fig.2. Loosely coupled integration approach

The error state dynamic equation is given by [14]:

$$\dot{\mathbf{x}} = \mathbf{F}\mathbf{x} + \mathbf{G}\mathbf{w} \quad (25)$$

where, \mathbf{x} is the system state ($n \times 1$) vector defined in equation (8), \mathbf{F} is the system dynamic ($n \times n$) matrix, \mathbf{w} is the system noise ($m \times 1$) vector and \mathbf{G} is the system noise ($n \times m$) matrix. For these equations the number of states $n = 18$ and the number of measurements $m = 6$. The elements of the error state dynamic equation can be described by [9]:

$$\mathbf{F} = \begin{bmatrix} \mathbf{F}_{rr} & \mathbf{F}_{rv} & \mathbf{0} & \mathbf{0} & \mathbf{0} \\ \mathbf{F}_{vr} & \mathbf{F}_{vv} & (\mathbf{f}^n \times) & \mathbf{C}_v^n \mathbf{L} \boldsymbol{\Omega} & -\frac{1}{2\sqrt{2}} \cdot \mathbf{C}_v^n \cdot \mathbf{J}_2 \\ \mathbf{F}_{er} & \mathbf{F}_{ev} & -(\boldsymbol{\omega}_{in}^n \times) & -\mathbf{C}_v^n & \mathbf{0} \\ \mathbf{0} & \mathbf{0} & \mathbf{0} & \mathbf{0} & -\frac{1}{2\sqrt{2}} \cdot \mathbf{L} \cdot \mathbf{J}_1 \\ \mathbf{0} & \mathbf{0} & \mathbf{0} & \mathbf{0} & \mathbf{0} \end{bmatrix} \quad (26)$$

$$\mathbf{G} = \begin{bmatrix} \mathbf{0} & \mathbf{0} \\ \frac{1}{2\sqrt{2}} \cdot \mathbf{C}_v^n \cdot \mathbf{J}_2 & \mathbf{0} \\ \mathbf{0} & \mathbf{0} \\ \frac{1}{2\sqrt{2}} \cdot \mathbf{J}_1 & \mathbf{0} \\ \mathbf{0} & \mathbf{I} \end{bmatrix} \quad (27)$$

$$\mathbf{w} = \begin{bmatrix} \mathbf{w}_a \\ \mathbf{w}_b \end{bmatrix} \quad (28)$$

The measurement equation is formulated as the difference of position and velocity computed by INS algorithm and given by GPS measurements:

$$\mathbf{z} = \mathbf{H}\mathbf{x} + \mathbf{v} \quad (29)$$

where,

$$\mathbf{z}_k = \begin{bmatrix} \mathbf{r}_{INS}^n - \mathbf{r}_{GPS}^n \\ \dots \\ \mathbf{v}_{INS}^n - \mathbf{v}_{GPS}^n \end{bmatrix} \quad (30)$$

$$\mathbf{H} = \begin{bmatrix} \mathbf{I}_{(3 \times 3)} & \mathbf{0}_{(3 \times 3)} & \mathbf{0}_{(3 \times 12)} \\ \mathbf{0}_{(3 \times 3)} & \mathbf{I}_{(3 \times 3)} & \mathbf{0}_{(3 \times 12)} \end{bmatrix}_{(6 \times 18)} \quad (31)$$

$$\mathbf{R} = \text{diag}(\sigma_{\phi}^2, \sigma_{\lambda}^2, \sigma_h^2, \sigma_{v_N}^2, \sigma_{v_E}^2, \sigma_{v_D}^2) \quad (32)$$

here \mathbf{z} is the measurements ($m \times 1$) vector, \mathbf{H} is the observation ($m \times n$) matrix, \mathbf{v} is the measurements noise ($m \times 1$) vector with $\mathbf{v} = N(0, \mathbf{R})$, and \mathbf{R} is the observation noise covariance ($m \times m$) matrix and its values are given by typical GPS signal processing errors.

4. SIMULATION RESULTS

Simulation is accomplished by providing the desired vehicle angular and linear accelerations on IMU, \mathbf{f}_{nom}^v and $\dot{\boldsymbol{\omega}}_{iv nom}^v$, as shown by Figure 3 and 4. Note the additional integration necessary to compute the angular velocity vector, due to the absence of gyroscopes.

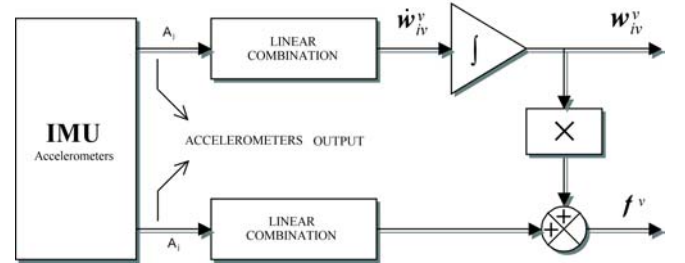


Fig.3. Gyro-free IMU computation scheme

The gyro-free IMU computation scheme is the inverse solution of equations (1) and (2):

$$\mathbf{A}_j = \mathbf{J}^{-1} \cdot \mathbf{k}_j \quad (33)$$

with $j = 1, \dots, 6$ and \mathbf{A}_j is the deterministic IMU output, and

$$\mathbf{k}_j = \begin{Bmatrix} 2\sqrt{2} \cdot \mathbf{L} \cdot \dot{\boldsymbol{\omega}}_{iv}^v \\ \dots \\ 2\sqrt{2} \cdot \left\{ \mathbf{f}^v - \mathbf{L} \cdot \begin{Bmatrix} \omega_Y \cdot \omega_Z \\ \omega_Z \cdot \omega_X \\ \omega_X \cdot \omega_Y \end{Bmatrix} \right\} \end{Bmatrix} = \mathbf{J} \cdot \mathbf{A} \quad (34)$$

$$\mathbf{J} = \begin{bmatrix} 1 & -1 & 0 & 0 & 1 & -1 \\ -1 & 0 & 1 & -1 & 0 & -1 \\ 0 & 1 & -1 & -1 & 1 & 0 \\ 1 & 1 & 0 & 0 & -1 & -1 \\ -1 & 0 & 1 & -1 & 0 & 1 \\ 0 & 1 & 1 & 1 & 1 & 0 \end{bmatrix} \quad (35)$$

For simulation purposes some error is added into equation (33) in order to characterize accelerometers bias and scale factor errors and noise [9]:

$$\hat{\mathbf{A}}_j = \mathbf{A}_j + \delta s r_j \cdot \mathbf{A}_j + \delta b r_j + \text{war}_j \quad (36)$$

where:

$\hat{\mathbf{A}}_j$ = is the real j^{th} accelerometer output

$\delta s r_j$ = denotes the scale factor error

$\delta b r_j$ = denotes the bias error

war_j = denotes the accelerometer noise

The IMU output, the measured \mathbf{f}^v and $\dot{\boldsymbol{\omega}}_{iv}^v$, are then used to compute the navigation solution given by equations (5), (6) and (7) as shown by Figure 4.

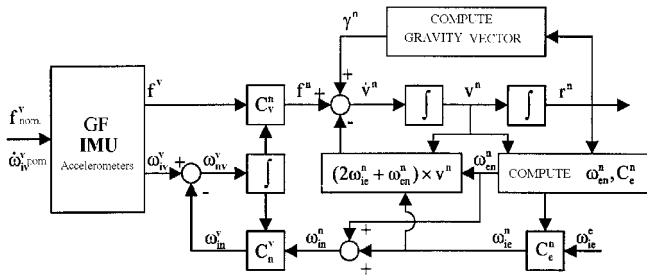


Fig.4. GF-IMU/INS mechanization

In order to simulate the system, the GPS accuracy measurements values are taken as $\pm 30\text{m}$ for height and $\pm 5 \cdot 10^{-6}$ rad for latitude and longitude. It is assumed that accelerometers are automotive low-cost type, manufactured in large scale with $20 \cdot 10^3$ (μg) bias, 2000 (ppm) scale factor and 325 ($\mu\text{g}/\text{Hz}^{1/2}$) noise. The IMU/INS system is simulated at 100 Hz and corrected at 1 Hz with measurements updates provided by GPS. The following figures show the simulations.

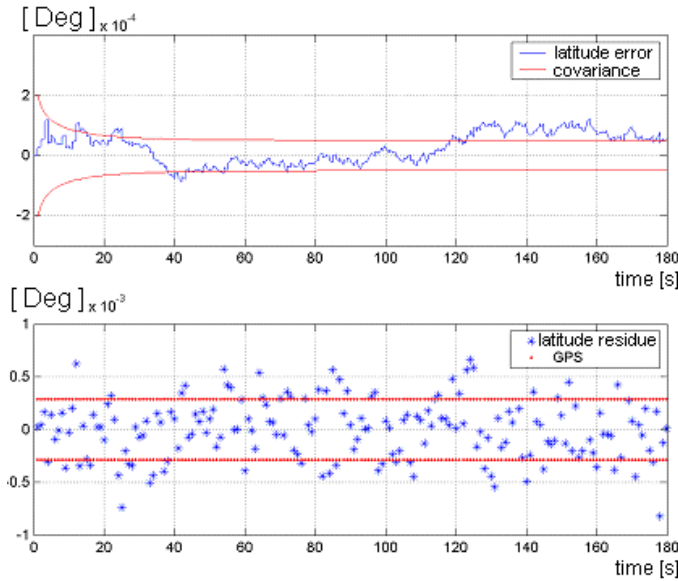


Fig.5. Error and residue for latitude measurements

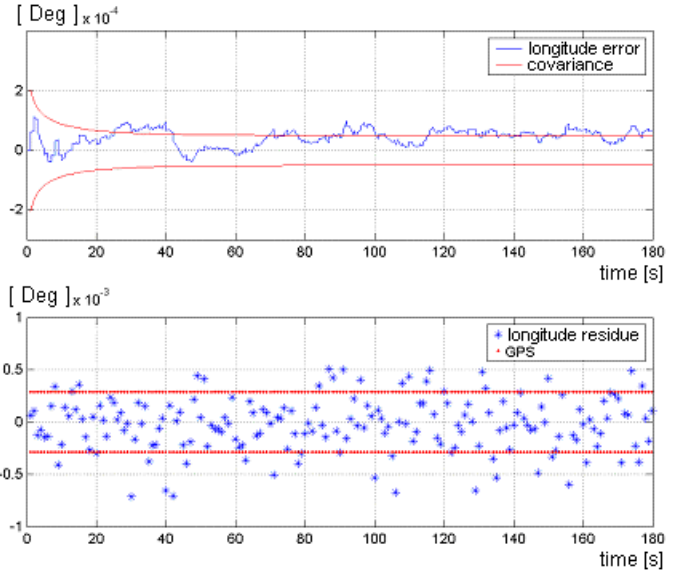


Fig.6. Error and residue for longitude measurements

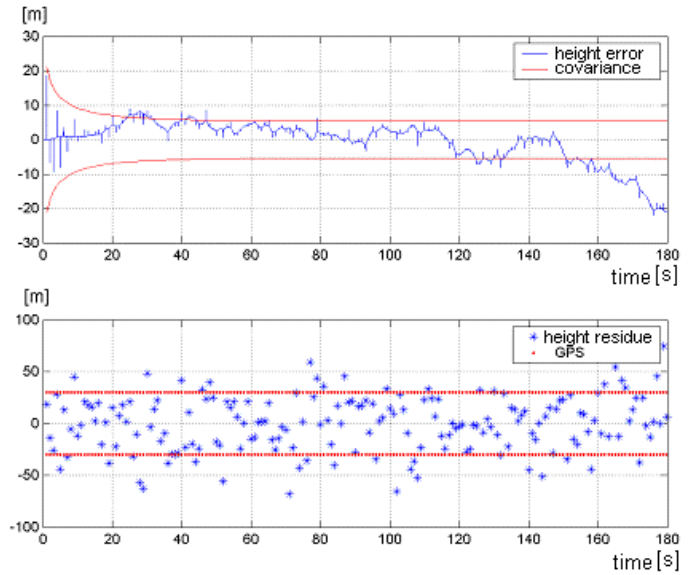


Fig.7. Error and residue for height measurements

Figures 5, 6 and 7 show error curves (nominal value – filtered values) plotted jointly with the errors standard deviations estimated by the filter. The residue curves, $(\mathbf{z} - \mathbf{H} \cdot \bar{\mathbf{x}})$, are plotted with $\pm \sigma_{\text{GPS}}$, the respective GPS measurements standard deviations, and $\bar{\mathbf{x}}$ denotes the propagated state vector.

After a transient period it can be noted that the errors due to the filter are most of the time confined within $\pm 1\sigma$, showing a procedure statistical consistency. Also, the residues were distributed around zero and confined within $\pm 1\sigma$ from GPS accuracy.

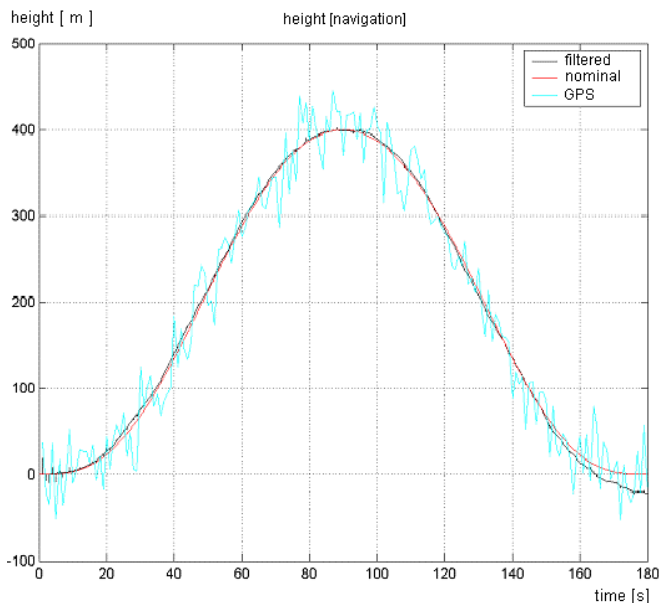


Fig.6. Nominal, filtered and GPS height curves

5. CONCLUSIONS

A non-standard strapdown inertial measurement unit with six accelerometers only and integrated GPS has been analyzed for low cost applications and low-medium performance. The cube type gyroscope free IMU was integrated with GPS data by using the Kalman filter.

An accelerometer lumped error model was presented, where scale factor and bias errors was concentrated in just one parameter modeled as white noise. This model reduces the system state to a 18x1 vector order.

The loosely coupled INS/GPS approach has shown to be sufficient to keep the filtered navigation solution limited by one standard deviation from GPS measurements. Also the simulation results confirm that the integrated navigation solution has better performance than the individual solutions from GPS and INS.

REFERENCES

- [1] Yazdi, N.; Ayazi, F.; Najafi, K. Micromachined inertial sensors. *Proceedings of the IEEE*, v. 86, n. 8, p. 1640-1659, ago. 1998.
- [2] El-Sheimy, N.; Integrated systems and their impact on the future of positioning, navigation and mapping applications. FIG working week 2000, Prage. 2000 Available at: <www.ddl.org/figtree/pub/proceedings/prague-final-papers/Papers-acrobats/el-sheimy-fin.pdf>. Accessed Jan. 2003.
- [3] Padgaonkar, A. J.; Krieger, K. W.; King, A. I. Measurement of angular acceleration of a rigid body using linear accelerometers. *Journal of Applied Mechanics, Transaction of the American Society of Mechanical Engineers*, v. 42, p. 552-556, Sep. 1975.
- [4] Merhav, S. J.; A non-gyroscopic inertial measurement unit. *Journal of Guidance and Control*, v. 5, n. 3, p. 227-235, 1982.
- [5] Trabasso, L. G.; Anteprojeto de uma unidade de medida inercial não giroscópica. São José dos Campos SP. 112p. (INPE-3887-TDL/220). Master Dissertation (Mestrado em Ciência Espacial/Mecânica Orbital), INPE-Instituto Nacional de Pesquisas Espaciais, 1986.
- [6] Chen, J. H.; Lee, S. C.; Debra, D. B. Gyroscope free strapdown inertial measurement unit by six linear accelerometers. *Journal of Guidance, Control and Dynamics*, v. 17, n. 2, p. 286-290, mar. 1994.
- [7] Mostov, K. S.; Soloniev, A. N.; Soloniev A. A. Accelerometer-based gyro-free multi-sensor INS. p. 245-254, 1998. *Proceedings of the ION, 54th Annual Meeting*.
- [8] Park, S.; Tan, C. W. GPS-aided gyroscope-free inertial navigation systems. California PATH research report. 2002 Available at: <www.path.berkeley.edu/PATH/research/>. Accessed Jan. 2003.
- [9] Marques Filho, E. A.; Navegação através de um sistema integrado GPS-INS baseado em IMU não-giroscópica. São José dos Campos S.P. (to be published). Master Dissertation (Mestrado em Engenharia e Tecnologia Espaciais), INPE-Instituto Nacional de Pesquisas Espaciais, 2005.
- [10] Titterton, D. H.; Weston, J. L. Strapdown inertial navigation technology. London: Peter Peregrinus Ltd., 1997. 455 p.
- [11] Britting, K. R.; Inertial navigation systems analysis. Massachusetts: John Wiley & Sons, Inc., 1971. 249 p.
- [12] Farrel, J. A.; Barth M. The global positioning system and inertial navigation. : McGraw-Hill, 1998. 340 p.
- [13] Grewal M. S.; Weill L. R.; Andrews A. P. Global positioning systems, inertial navigation and integration. John Wiley and Sons Ltd, 2001. 392 p.
- [14] Brown, R. G.; Hwang, P. Y. C. Introduction to random signals and applied Kalman filtering: with MATLAB exercises and solutions. : John Wiley and Sons, 1997. 484 p.